

This is the accepted manuscript made available via CHORUS. The article has been published as:

Topological Magnon Bands and Unconventional Superconductivity in Pyrochlore Iridate Thin Films

Pontus Laurell and Gregory A. Fiete

Phys. Rev. Lett. **118**, 177201 — Published 26 April 2017

DOI: [10.1103/PhysRevLett.118.177201](https://doi.org/10.1103/PhysRevLett.118.177201)

Topological magnon bands and unconventional superconductivity in pyrochlore iridate thin films

Pontus Laurell* and Gregory A. Fiete

Department of Physics, The University of Texas at Austin, Austin, TX 78712, USA

We theoretically study the magnetic properties of pyrochlore iridate bilayer and trilayer thin films grown along the [111] direction using a strong coupling approach. We find the ground state magnetic configurations on a mean field level and carry out a spin-wave analysis about them. In the trilayer case the ground state is found to be the all-in/all-out (AIAO) state, whereas the bilayer has a deformed AIAO state. For all parameters of the spin-orbit coupled Hamiltonian we study, the lowest magnon band in the trilayer case has a non-zero Chern number. In the bilayer case we also find a parameter range with non-zero Chern numbers. We calculate the magnon Hall response for both geometries, finding a striking sign change as function of temperature. Using a slave-boson mean-field theory we study the doping of the trilayer system and discover an unconventional time-reversal symmetry broken $d+id$ superconducting state. Our study complements prior work in the weak coupling limit and suggests that the [111] grown thin film pyrochlore iridates are a promising candidate for topological properties and unconventional orders.

PACS numbers: 75.25.-j, 75.30.Ds, 71.27.+a

Introduction - One of the main focal points of quantum materials research is topological states of matter, where the essential physics is generally due to spin-orbit coupling (SOC) [1–4]. Another is correlated electron systems, in which electron-electron interactions dominate, leading to interaction-driven insulators, magnetism, and unconventional superconductivity [5]. Even more possibilities open up when both SOC and electron-electron interactions are present, such as fractionalized topological insulators (TI) [6–17], interaction-induced TI [18–24], and unconventional magnetic states [25–27]. A promising place to look for both types of physics is in $5d$ transition-metal oxides, which tend to have comparable electron-electron interaction and SOC strengths [28–30].

Among these, the pyrochlore iridates $A_2\text{Ir}_2\text{O}_7$ (where A is a rare earth element) have seen a lot of interest [8, 10, 11, 16, 31–35], in part due to the geometrically frustrated lattice suggesting exotic magnetic phenomena such as chiral spin liquids [36], and in part since some iridates allow an elegant treatment of the iridium orbitals in the form of a single effective $j_{eff} = 1/2$ moment [37–40]. (The splitting of the t_{2g} orbitals into separate $j = 1/2$ and $j = 3/2$ manifolds may be violated in practice, but still represents a good starting point unless one intends to make quantitatively accurate first-principles predictions [41, 42].) Magnetically, the bulk systems tend to order in a noncollinear $q = 0$ all-in/all-out (AIAO) configuration [42–47], although $\text{Pr}_2\text{Ir}_2\text{O}_7$ shows no signs of order at the lowest experimentally accessible temperatures [48, 49]. As for electronic phases, there are many theoretical possibilities, including axion insulators [32, 34, 50], topological Mott insulators [11, 16], topological crystalline insulators [10], other varieties of correlated topological insulators [8], and Weyl semimetals [31, 32, 34, 51]. Thin films grown along high symmetry directions have been shown to offer further possible phases, that are not readily inferred from the bulk ones [41, 52–56].

Previous thin film studies have approached the system from the weak coupling limit [41, 57], but the materials are really in the non-perturbative intermediate coupling regime [28–

30]. Here we describe work starting from the strong-coupling limit, offering a perspective complementary to previous studies. Alternatively, one can view our work as a study of spin (local moment) models with SOC on decorated kagome lattices, possibly artificially created in an optical lattice using artificial gauge fields to realize the SOC and spin interaction terms [58–61]. While experiments on $\text{Eu}_2\text{Ir}_2\text{O}_7$ provide evidence for an AIAO order in thicker thin films [62–64], theoretical studies on atomically thin bilayers and trilayers are less conclusive [41, 52, 53]. We find that, in the strong coupling limit and on the mean field level, the magnetic ground state is AIAO in the trilayer system, and closely related to it in the bilayer. Performing a spin-wave analysis about the magnetic ground state, we find the lowest energy band is isolated and has a non-zero Chern number. We calculate the associated (thermal) magnon Hall response, which shows strong signatures of the band topology. Finally we introduce dopants into the system, and explore the phase diagram in a slave-boson mean field treatment, discovering that a large region of parameter space hosts an unconventional time-reversal symmetry broken $d + id$ superconducting phase in which the order parameter sign alternates between layers.

Spin model - The spin Hamiltonian for the bulk system is [65]

$$H = \sum_{ij} \left[JS_i \cdot S_j + \mathbf{D}_{ij} \cdot (\mathbf{S}_i \times \mathbf{S}_j) + S_i^a \Gamma_{ij}^{ab} S_j^b \right], \quad (1)$$

where \mathbf{S}_i is the effective spin-1/2 moment on site i , and the terms represent the antiferromagnetic (AF) Heisenberg coupling, Dzyaloshinskii-Moriya (DM) interaction (DMI) and symmetric anisotropic exchange, respectively. The latter two are given in terms of the normalized DM vectors \hat{v}_{ij} [31], by $\mathbf{D}_{ij} = DM\hat{v}_{ij}$ and $\Gamma_{ij}^{ab} = \Gamma(\hat{v}_{ij}^a \hat{v}_{ij}^b - \delta^{ab}/3)$, parametrized by the strengths DM and Γ , respectively. In the strong coupling limit, the three interaction strengths can be determined microscopically using a Slater-Koster (SK) approach [31, 33]. In the simplest models they are functions of the SK parameter t_σ with an overall scaling due to the Hubbard U coupling

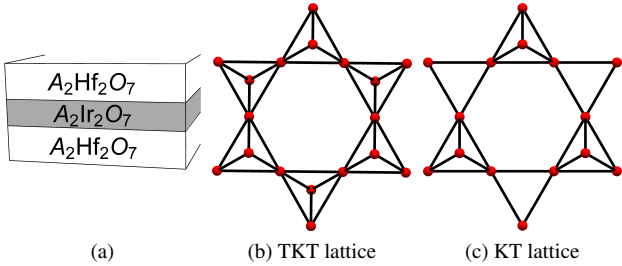


FIG. 1. (color online) (a) ‘‘Sandwich’’ structure. (b) Top view of trilayer grown along [111]. (c) Top view of bilayer structure.

[31, 33]. It is also possible to determine the direction of the DM vectors (up to an overall sign) from symmetry alone [66–68], producing two configurations known as direct and indirect, associated with an AIAO order and a noncoplanar order, respectively. For bulk pyrochlore iridates, the direct configuration is expected and there is indeed also direct experimental evidence for the AIAO order [45].

In this work we focus on thin films of pyrochlore iridates with non-magnetic A site ions [69] grown [70] in the [111] direction [41, 52–56]. Along this axis, the pyrochlore lattice consists of alternating triangular and kagome layers. We focus on triangular-kagome-triangular (TKT) trilayers and kagome-triangular (KT) bilayers [41, 52, 53], as shown in Fig. 1. It is assumed that the spin Hamiltonian for these layers is the same as in the bulk case, but that the lattice develops inequivalent sublattices with different coordination numbers. For example, in the TKT case sites in the triangular (kagome) layers have 3 (6) nearest neighbors (NNs). The absence of a mirror plane means that we are unable to determine the thin film DM vectors from Moriya’s rules. Instead, we take them to be inherited from the bulk lattice [69]. To this end, and to minimize distortion effects, we consider a ‘‘sandwich structure’’ with lattice matched support layers, as shown in Fig. 1(a).

Following bulk results [34, 66] as well as thin film predictions [41, 52–55], we assume a $\mathbf{q} = 0$ (translationally invariant) structure and solve the model variationally on the mean-field level. In the case of the TKT trilayer, we generically find the AIAO state, as shown in Fig. 2a. In the KT bilayer case, the symmetry is lowered even further, and we find a family of distorted AIAO states. Essentially, these are spin configurations similar to the AIAO structure, but the spins do not meet in the center of the tetrahedron. The z coordinate of this intersection point can be used to classify the magnetic configuration and measure how far from the AIAO state it is. A typical case is shown in Fig. 2b. However, if we set $J = 1$ and choose $DM < 0$ and Γ freely, eschewing direct ties to microscopic models, we find that it is possible to get arbitrarily close to the AIAO state [69].

Reaching the AIAO state in the bilayer does require a fine-tuning of both DM and Γ , as well as an unusually high value for the DM strength with $|DM|/J \gtrsim 1$, whereas experiments suggest $|DM|/J \sim 0.1–0.3$ [46]. Nevertheless, it is interesting

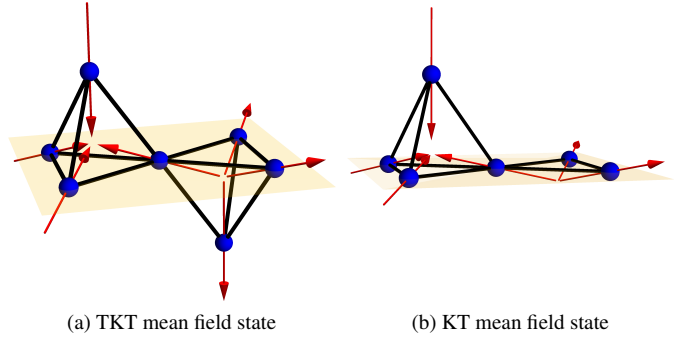


FIG. 2. (color online) (a) The AIAO structure generically found on for the TKT trilayer, and (b) the deformed AIAO state typical for the KT bilayer. The shaded planes represents the Kagome plane.

to consider these bilayer mean field states proximate to the AIAO order for $|DM|/J \geq 0.7$ as they yield topological lowest magnon bands, whereas those found for the parameters used in the TKT case do not. In addition, we note that optical lattice systems may allow strengths up to $|DM|/J = 1$ [61], rendering our work potentially relevant to those experimental systems.

Topological magnon bands - To study spinwaves in non-collinear magnetic structures, we first perform a sublattice dependent rotation to make the local z -axis point in the direction of the local moment, and then introduce a Holstein-Primakoff representation [71]. The resulting Hamiltonian is truncated to quadratic order, Fourier transformed and then diagonalized using a Bogoliubov transform [72]. The magnon spectra for bulk pyrochlore iridates was studied in Ref. [73], employing a parametrization in which

$$J = \frac{4t^2}{U} \left[\cos^2 \left(\frac{\theta_t}{2} - \theta \right) - \frac{1}{3} \sin^2 \left(\frac{\theta_t}{2} - \theta \right) \right], \quad (2)$$

$$\mathbf{D}_{ij} = \frac{8t^2}{U} \cos \left(\frac{\theta_t}{2} - \theta \right) \sin \left(\frac{\theta_t}{2} - \theta \right) \hat{v}_{ij}, \quad (3)$$

$$\Gamma_{ij}^{ab} = \frac{8t^2}{U} \sin^2 \left(\frac{\theta_t}{2} - \theta \right) \left[\hat{v}_{ij}^a \hat{v}_{ij}^b - \frac{\delta^{ab}}{3} \right], \quad (4)$$

where $\theta_t = 2 \arctan \sqrt{2} \approx 109.47^\circ$ is the tetrahedral angle. In this parametrization it is clear that energies scale by t^2/U , and θ is the parameter determining the relative importance of the interactions. The system approaches the Heisenberg limit and becomes gapless as $\theta \rightarrow \theta_t/2 \approx 0.96$. In the bulk system, the cubic symmetry guarantees a threefold degeneracy at the Γ point [73]. This degeneracy is lifted in the thin film case, and we generically find an isolated lowest band, as can be seen in Figs. 3a and 3c, for the trilayer and bilayer systems, respectively. Since the lowest band is isolated, it has a well-defined (first) Chern number, which we calculate numerically using the Fukui method [74]. It turns out to be non-zero in a large portion of the parameter space, due to the noncoplanar spin texture, caused by the DM and Γ terms, inducing a non-trivial Berry phase on magnon motion through the Brillouin zone. The relatively flat band also implies that magnon-magnon interactions could lead to correlated boson (magnon) behavior.

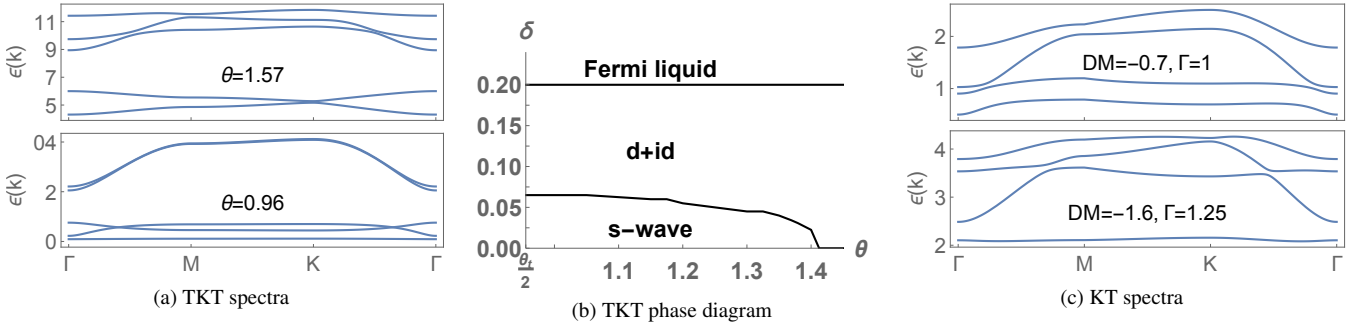


FIG. 3. (color online) (a) Spin-wave spectra in the trilayer system for the DMI-dominated case $\theta = 1.57$ and approaching the Heisenberg limit at $\theta \approx 0.96$. Energies are given in units of t^2/U (b) Phase diagram for the t-J-like model in the trilayer system. (c) Spin-wave spectra in the bilayer system for a topologically non-trivial case $DM = -0.7$, and $DM = -1.6$, which is trivial. Energies are given in units of the Heisenberg coupling J .

In the TKT spectra (Fig. 3a) we use the parametrization given above, and find that the direct gap between the two lowest bands is $0.114t^2/U$ ($0.135t^2/U$) for $\theta = 1.57$ ($\theta = 0.96$). Taking $\text{Y}_2\text{Ir}_2\text{O}_7$ as a typical example of a Mott-insulating AIAO magnet, we have the realistic value $U = 2.5\text{eV}$ from first-principles calculations on the bulk material [42]. Assuming $U/t = 6$, the smaller gap is 92K . Since the iridates are most likely in the intermediate coupling regime, the U/t ratio is unlikely to be significantly higher. The gap should thus correspond to experimentally accessible temperatures away from a band closing at $\theta_c = 1.26$. Defining the flatness ratio as band gap over bandwidth, the TKT bands (apart from the $\theta = 0.96$ case which approaches the Heisenberg limit) have flatness ratios on the order of $1/10$ [69]. Throughout the parameter space considered, the lowest band has a non-zero Chern number $C = \pm 1$, with a topological transition at θ_c . The full band evolution is shown in the supplemental material [69].

For the KT spectra (Fig. 3c) we used values of DM/J and Γ/J chosen to engineer a state as close to the AIAO order as possible. Again, we stress that iridates are unlikely to reach the high DM strength required, but it might be possible to engineer in optical lattice systems. Supposing that is the case, we find that the gap closes around $DM/J = -1.3$, representing a topological transition from $C = -1$ at $|DM| < 1.3$ to a topologically trivial system for $|DM| > 1.3$ [69]. In the topological sector, the gap is $0.3J \approx 95\text{K}$, using $J = 27.3(6)\text{meV}$ as reported for $\text{Sm}_2\text{Ir}_2\text{O}_7$ [46], giving a flatness ratio that is approximately one. In general we seem unable to achieve a both very flat and topologically non-trivial band in these systems, which would allow for interesting interaction effects [75]. Including longer-range interactions (which translate into longer range hopping terms for the spin waves) could perhaps change that, as in the case of electronic Chern insulators [76].

Since magnons are bosonic excitations, a quantized magnetic (thermal) Hall response is not expected. Instead we envision the kind of observations found in other topological bosonic systems [77], such as photonic topological insulators [78], Hofstadter bands in ultra cold bosonic atoms [79], topological bands in cold bosonic atoms [80], and topological po-

lariton insulators [81, 82]. Wave packets are excited into the non-trivial bands, possibly using a pulsed magnetic field as a pump, producing long-lived edge excitations.

We have also computed (see Fig.4) a magnon Hall effect, in which the magnon edge current produces a thermal Hall current in the presence of a temperature gradient and an associated transverse thermal conductivity κ_{xy} [83–86]. As a function of temperature, we find [69] a sign change in κ_{xy} that reflects the topological nature of the thermal Hall effect in this system as bands of different Chern number come to dominate the transverse thermal transport [87]. Observing this sign change requires a sensitivity of $\approx 10^{-10} \text{ W/K}$ [69]. The thermal Hall effect has been experimentally demonstrated in collinear pyrochlore and kagome ferromagnets [88–93], and predicted to occur also in kagome antiferromagnets [94–96], as well as other systems [97–101]. The topology is due to the DMI in collinear systems, and finite spin chirality of the magnetic order in non-coplanar systems, which may be caused by DMI or magnetic fields. To our best knowledge, the current study is the first to predict it will occur in this specific non-collinear/non-coplanar magnetic configuration. The non-collinearity makes the order more susceptible to control by external magnetic fields. For small fields we expect the thermal Hall conductivity should still be present since the lowest magnon band is separated by a gap from the next higher band.

Doping and superconductivity - To identify order parameters with the same symmetries as the spin Hamiltonian, we first employ a hidden symmetry [102] to write the Hamiltonian, Eq.(1), in a Heisenberg form, $H = \sum_{ij} J_0 \mathbf{S}'_i \cdot \mathbf{S}'_j$, where the site- and bond-dependent SO(3) transformation depends on the normalized DM vector $\hat{\mathbf{v}}_{ij}$ according to,

$$\mathbf{S}'_k = (1 - \cos \phi) (\hat{\mathbf{v}}_{ij} \cdot \mathbf{S}_k) \hat{\mathbf{v}}_{ij} + \cos \phi \mathbf{S}_k - \sin \phi \mathbf{S}_k \times \hat{\mathbf{v}}_{ij}, \quad (5)$$

where $\phi_k = \phi(\delta_{ki} - \delta_{kj})$. The angle ϕ can be related to the θ parameter used in the spin wave parametrization through $\phi = \theta_i/2 - \theta$. Using the methods of Refs. [103 and 104], we next represent the rotated spin operators by fermionic spinons f_σ

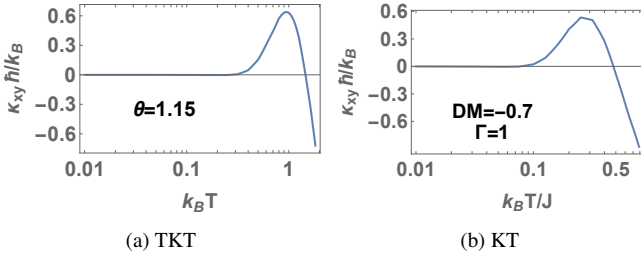


FIG. 4. Temperature dependence of the magnon Hall conductivity, $K_{xy}(T)$ for (a) the TKT trilayer system and (b) the KT bilayer system, up to the estimated ordering temperature [69]. The sign change of the thermal Hall conductivity with temperature is associated with a change in which topological bands dominate the transport [69]. In (a) $k_B T$ is given in units of t^2/U .

through $S_i^{ra} = \frac{1}{2} f_{i\sigma}^\dagger \tau_{\sigma\sigma'}^a f'_{i\sigma'}$, subject to the local constraint [5] $\sum_\sigma f_{i\sigma}^\dagger f'_{i\sigma} = 1$, which will later be approximated by a global constraint for each sublattice. We identify the usual t-J model order parameters for spin-conserving exchange, $\hat{\chi}'_{ij} = f'_{ia}^\dagger f'_{ja}$ and singlet pairing, $\hat{\Delta}'_{ij} = f'_{ia} i \tau_{\alpha\beta}^y f'_{jb} = f'_{i\uparrow} f'_{j\downarrow} - f'_{i\downarrow} f'_{j\uparrow}$. These order parameters are then rotated back to the original coordinate system using a SU(2) transformation. This procedure gives us the parameters [69],

$$\hat{\chi}_{ij} = f_{i\alpha}^\dagger f_{j\alpha}, \quad \hat{\psi}_{ij} = f_{i\alpha}^\dagger (i \hat{v}_{ij} \cdot \vec{\tau})_{\alpha\beta} f_{j\beta}, \quad (6)$$

$$\hat{\Delta}_{ij} = f_{i\alpha} i \tau_{\alpha\beta}^y f_{j\beta}, \quad \hat{\xi}_{ij} = f_{i\alpha} (\tau^y \hat{v}_{ij} \cdot \vec{\tau})_{\alpha\beta} f_{j\beta}, \quad (7)$$

representing spin-conserving exchange, non-spin-conserving exchange, singlet and triplet pairing, respectively. Similar order parameters have been employed for Kitaev-Heisenberg models [105, 106], but in our model the components of the non-spin-conserving exchange and triplet pairing parameters get weighted by the DM vectors. This is a reflection of the spin-lattice coupling due to the the DM interaction, and the effect vanishes in the absence of spin-orbit coupling, as seen in the relations [69],

$$\hat{\chi}'_{ij} = \cos(\theta_t/2 - \theta) \hat{\chi}_{ij} + \sin(\theta_t/2 - \theta) \hat{\psi}_{ij}, \quad (8)$$

$$\hat{\Delta}'_{ij} = \cos(\theta_t/2 - \theta) \hat{\Delta}_{ij} - \sin(\theta_t/2 - \theta) \hat{\xi}_{ij}, \quad (9)$$

where $\theta = \theta_t/2$ for the Heisenberg case, as before.

Dopants are introduced through a hopping term $H_t = -t \sum_{\langle ij \rangle \sigma} (c_{i\sigma}^\dagger c_{j\sigma} + \text{H.c.})$, where c^\dagger is an electron or hole creation operator (our treatment is symmetric in this respect). To disallow double occupation this fermion operator is represented as $c_{i\sigma}^\dagger = f_{i\sigma}^\dagger b_i$, where b is the slave-boson operator subject to the constraint $1 = b_i^\dagger b_i + \sum_\sigma f_{i\sigma}^\dagger f_{i\sigma}$. We assume that all bosons are condensed in their lowest band, i.e. $\delta = \langle b_i^\dagger b_i \rangle = \langle b_i^\dagger b_j \rangle$, which holds in the low-doping regime at zero temperature. This leads us to the mean-field hopping term $H_t = -t\delta \sum_{\langle ij \rangle} (f_{i\sigma}^\dagger f_{j\sigma} + \text{H.c.})$. We further carry out mean-field decouplings for all our order parameters, assuming one value per sublattice. This results in a system of

36 mean-field parameters to be solved self-consistently [69]. To make the problem more tractable, we introduce ansatzes for *s*- and time-reversal symmetry breaking *d*-wave states. In both cases we distinguish between bonds between sites both located in the kagome plane (in-plane bonds), and bonds between a site in the kagome plane and a site in a triangular layer (out-of-plane bonds). These are necessarily different, as in- and out-of-plane sites have different coordination numbers. We also take the exchange order parameters $\chi_{in}, \chi_{out}, \psi_{in}$ and ψ_{out} to be real-valued and the triplet pairing order parameter to be zero. In the *s*-wave ansatz, the singlet pairing parameter satisfies $\Delta = (\Delta_{in}, \Delta_{in}, \Delta_{out}, \Delta_{out})$. In the *d* + *id*-wave ansatz, $\Delta = (\Delta_{in}, \Delta_{in} e^{i2\pi/3}, \Delta_{out} e^{i\pi/3}, \Delta_{out} e^{i\pi/3})$ [69].

The results of the self-consistent calculations are shown in Fig. 3b. At low doping δ and spin-orbit coupling we find the *s*-wave ansatz to be energetically favorable. There is a transition to the *d* + *id*-wave state at finite doping, the value of which decreases with increased spin-orbit strength. Over $\delta \approx 0.2$ the superconducting order parameter vanishes, leading to a Fermi liquid state. In both the *s*- and *d* + *id*-wave solutions the self-consistent results have the order parameter changing sign between in-plane and out-of-plane bonds, i.e. $\text{sgn}(\Delta_{out}) = -\text{sgn}(\Delta_{in})$. This kind of sign change can be understood by analogy to layered superconductors, where non-centrosymmetry can induce Rashba SOC with signs that alternate between layers, driving a similar sign change of the order parameter [107–109]. While our model does not explicitly contain a Rashba-like term, spin-orbit physics is present in the form of DM and Γ interactions. These, in turn, drive a magnetic order, the moments of which can be considered analogues of the effective magnetic field due to the Rashba effect. Considering the AIAO order of Fig. 2a, one finds that the in-plane moments can be averaged to an effective field $\mathbf{B}_{eff} \sim +\hat{z}$. Similarly the out-of-plane moments have $\mathbf{B}_{eff} \sim -\hat{z}$, which yields the same kind of sign structure.

Conclusion - In this letter we have shown, using a strong coupling (local moment) model, that thin film pyrochlore iridates are expected to exhibit topological magnon bands, with strong signatures in the temperature dependence of the thermal conductivity, as well as exotic time-reversal symmetry broken *d* + *id* superconductivity upon doping. We focused on the ultra thin bilayer and trilayer systems grown in the [111] direction. Our work complements earlier studies that used the weak coupling limit as a starting point, and draws connections to layered superconductors and magnon Hall physics.

We thank Victor Chua, Bert Halperin, Rex Lundgren, and Allan H. MacDonald for helpful discussions. We gratefully acknowledge funding from grants ARO grant W911NF-14-1-0579 and NSF DMR-1507621. This work used the Extreme Science and Engineering Discovery Environment (XSEDE), which is supported by National Science Foundation grant number ACI-1053575, and the Texas Advanced Computing Center (TACC).

* laurell@physics.utexas.edu

-
- [1] X.-L. Qi and S.-C. Zhang, Rev. Mod. Phys. **83**, 1057 (2011).
- [2] M. Z. Hasan and C. L. Kane, Rev. Mod. Phys. **82**, 3045 (2010).
- [3] J. E. Moore, Nature **464**, 194 (2010).
- [4] Y. Ando, J. Phys. Soc. Jpn. **82**, 102001 (2013).
- [5] P. A. Lee, N. Nagaosa, and X.-G. Wen, Rev. Mod. Phys. **78**, 17 (2006).
- [6] M. Levin and A. Stern, Phys. Rev. Lett. **103**, 196803 (2009).
- [7] J. Maciejko and G. A. Fiete, Nat. Phys. **11**, 385 (2015).
- [8] J. Maciejko, V. Chua, and G. A. Fiete, Phys. Rev. Lett. **112**, 016404 (2014).
- [9] A. Rüegg and G. A. Fiete, Phys. Rev. Lett. **108**, 046401 (2012).
- [10] M. Kargarian and G. A. Fiete, Phys. Rev. Lett. **110**, 156403 (2013).
- [11] M. Kargarian, J. Wen, and G. A. Fiete, Phys. Rev. B **83**, 165112 (2011).
- [12] J. Maciejko and A. Rüegg, Phys. Rev. B **88**, 241101 (2013).
- [13] J. Maciejko, X.-L. Qi, A. Karch, and S.-C. Zhang, Phys. Rev. Lett. **105**, 246809 (2010).
- [14] J. Maciejko, X.-L. Qi, A. Karch, and S.-C. Zhang, Phys. Rev. B **86**, 235128 (2012).
- [15] A. Stern, Annu. Rev. Condens. Matter Phys. **7**, 349 (2016).
- [16] D. Pesin and L. Balents, Nat. Phys. **6**, 376 (2010).
- [17] M. W. Young, S.-S. Lee, and C. Kallin, Phys. Rev. B **78**, 125316 (2008).
- [18] S. Raghu, X.-L. Qi, C. Honerkamp, and S.-C. Zhang, Phys. Rev. Lett. **100**, 156401 (2008).
- [19] J. Wen, A. Rüegg, C.-C. J. Wang, and G. A. Fiete, Phys. Rev. B **82**, 075125 (2010).
- [20] C. Weeks and M. Franz, Phys. Rev. B **81**, 085105 (2010).
- [21] Y. Zhang, Y. Ran, and A. Vishwanath, Phys. Rev. B **79**, 245331 (2009).
- [22] K.-Y. Yang, W. Zhu, D. Xiao, S. Okamoto, Z. Wang, and Y. Ran, Phys. Rev. B **84**, 201104 (2011).
- [23] A. Rüegg and G. A. Fiete, Phys. Rev. B **84**, 201103 (2011).
- [24] Y. Wang, Z. Wang, Z. Fang, and X. Dai, Phys. Rev. B **91**, 125139 (2015).
- [25] M. Kargarian, A. Langari, and G. A. Fiete, Phys. Rev. B **86**, 205124 (2012).
- [26] J. Reuther, R. Thomale, and S. Rachel, Phys. Rev. B **86**, 155127 (2012).
- [27] J. G. Rau, E. K.-H. Lee, and H.-Y. Kee, Phys. Rev. Lett. **112**, 077204 (2014).
- [28] W. Witczak-Krempa, G. Chen, Y. B. Kim, and L. Balents, Annu. Rev. Condens. Matter Phys. **5**, 57 (2014).
- [29] J. G. Rau, E. K.-H. Lee, and H.-Y. Kee, Annu. Rev. Condens. Matter Phys. **7**, 195 (2016).
- [30] R. Schaffer, E. Kin-Ho Lee, B.-J. Yang, and Y. B. Kim, Rep. Prog. Phys. **79**, 094504 (2016).
- [31] W. Witczak-Krempa and Y. B. Kim, Phys. Rev. B **85**, 045124 (2012).
- [32] G. Chen and M. Hermele, Phys. Rev. B **86**, 235129 (2012).
- [33] W. Witczak-Krempa, A. Go, and Y. B. Kim, Phys. Rev. B **87**, 155101 (2013).
- [34] X. Wan, A. M. Turner, A. Vishwanath, and S. Y. Savrasov, Phys. Rev. B **83**, 205101 (2011).
- [35] B.-J. Yang and Y. B. Kim, Phys. Rev. B **82**, 085111 (2010).
- [36] Y. Machida, S. Nakatsuji, S. Onoda, T. Tayama, and T. Sakakibara, Nature **463**, 210 (2010).
- [37] B. J. Kim, H. Jin, S. J. Moon, J.-Y. Kim, B.-G. Park, C. S. Leem, J. Yu, T. W. Noh, C. Kim, S.-J. Oh, J.-H. Park, V. Durairaj, G. Cao, and E. Rotenberg, Phys. Rev. Lett. **101**, 076402 (2008).
- [38] B. J. Kim, H. Ohsumi, T. Komesu, S. Sakai, T. Morita, H. Takagi, and T. Arima, Science **323**, 1329 (2009).
- [39] J. Kanamori, Prog. Theor. Phys. **17**, 177 (1957).
- [40] H. Zhang, K. Haule, and D. Vanderbilt, Phys. Rev. Lett. **111**, 246402 (2013).
- [41] X. Hu, Z. Zhong, and G. A. Fiete, Sci. Rep. **5**, 1072 (2015).
- [42] H. Shinaoka, S. Hoshino, M. Troyer, and P. Werner, Phys. Rev. Lett. **115**, 156401 (2015).
- [43] S. M. Disseler, C. Dhital, A. Amato, S. R. Giblin, C. de la Cruz, S. D. Wilson, and M. J. Graf, Phys. Rev. B **86**, 014428 (2012).
- [44] H. Sagayama, D. Uematsu, T. Arima, K. Sugimoto, J. J. Ishikawa, E. O'Farrell, and S. Nakatsuji, Phys. Rev. B **87**, 100403 (2013).
- [45] S. M. Disseler, Phys. Rev. B **89**, 140413 (2014).
- [46] C. Donnerer, M. C. Rahn, M. M. Sala, J. G. Vale, D. Pincini, J. Stremper, M. Krisch, D. Prabhakaran, A. T. Boothroyd, and D. F. McMorrow, Phys. Rev. Lett. **117**, 037201 (2016).
- [47] T. Liang, T. H. Hsieh, J. J. Ishikawa, S. Nakatsuji, L. Fu, and N. P. Ong, “Orthogonal magnetization and symmetry breaking in pyrochlore iridate $\text{Eu}_2\text{Ir}_2\text{O}_7$,” (2016), arXiv:1603.08022.
- [48] S. Nakatsuji, Y. Machida, Y. Maeno, T. Tayama, T. Sakakibara, J. v. Duijn, L. Balicas, J. N. Millican, R. T. Macaluso, and J. Y. Chan, Phys. Rev. Lett. **96**, 087204 (2006).
- [49] G. Chen, Phys. Rev. B **94**, 205107 (2016).
- [50] A. Go, W. Witczak-Krempa, G. S. Jeon, K. Park, and Y. B. Kim, Phys. Rev. Lett. **109**, 066401 (2012).
- [51] K.-Y. Yang, Y.-M. Lu, and Y. Ran, Phys. Rev. B **84**, 075129 (2011).
- [52] X. Hu, A. Rüegg, and G. A. Fiete, Phys. Rev. B **86**, 235141 (2012).
- [53] Q. Chen, H.-H. Hung, X. Hu, and G. A. Fiete, Phys. Rev. B **92**, 085145 (2015).
- [54] B.-J. Yang and N. Nagaosa, Phys. Rev. Lett. **112**, 246402 (2014).
- [55] K. Hwang and Y. B. Kim, Sci. Rep. **6**, 30017 (2016).
- [56] E. J. Bergholtz, Z. Liu, M. Trescher, R. Moessner, and M. Udagawa, Phys. Rev. Lett. **114**, 016806 (2015).
- [57] G. A. Fiete and A. Ruegg, J. Appl. Phys. **117**, 172602 (2015).
- [58] J. Dalibard, F. Gerbier, G. Juzeliūnas, and P. Öhberg, Rev. Mod. Phys. **83**, 1523 (2011).
- [59] W. S. Cole, S. Zhang, A. Paramekanti, and N. Trivedi, Phys. Rev. Lett. **109**, 085302 (2012).
- [60] J. Radić, A. Di Ciolo, K. Sun, and V. Galitski, Phys. Rev. Lett. **109**, 085303 (2012).
- [61] M. Gong, Y. Qian, M. Yan, V. W. Scaola, and C. Zhang, Sci. Rep. **5**, 10050 (2015).
- [62] T. Fujita, Y. Kozuka, M. Uchida, A. Tsukazaki, T. Arima, and M. Kawasaki, Sci. Rep. **5**, 9711 (2015).
- [63] T. C. Fujita, M. Uchida, Y. Kozuka, S. Ogawa, A. Tsukazaki, T. Arima, and M. Kawasaki, Appl. Phys. Lett. **108**, 022402 (2016).
- [64] T. C. Fujita, M. Uchida, Y. Kozuka, W. Sano, A. Tsukazaki, T. Arima, and M. Kawasaki, Phys. Rev. B **93**, 064419 (2016).
- [65] K. A. Ross, L. Savary, B. D. Gaulin, and L. Balents, Phys. Rev. X **1**, 021002 (2011).
- [66] M. Elhajal, B. Canals, R. Sunyer, and C. Lacroix, Phys. Rev. B **71**, 094420 (2005).
- [67] T. Moriya, Phys. Rev. Lett. **4**, 228 (1960).
- [68] T. Moriya, Phys. Rev. **120**, 91 (1960).
- [69] See supplemental material [url], which includes Refs. [110–

- [115].
- [70] W. Yang, Y. Xie, W. Zhu, K. Park, A. Chen, Y. Losovyj, Z. Li, H. Liu, M. Starr, J. A. Acosta, C. Tao, N. Li, Q. Jia, J. J. Heremans, and S. Zhang, “Epitaxial thin films of pyrochlore iridate $\text{Bi}_{2+x}\text{Ir}_{2-y}\text{O}_{7-\delta}$: structure, defects and transport properties,” (2016), arXiv:1608.08608.
- [71] A. Auerbach, *Interacting Electrons and Quantum Magnetism* (Springer-Verlag, New York, 1994).
- [72] A. G. Del Maestro and M. J. P. Gingras, *J. Phys. Condens. Matter* **16**, 3339 (2004).
- [73] E. K.-H. Lee, S. Bhattacharjee, and Y. B. Kim, *Phys. Rev. B* **87**, 214416 (2013).
- [74] T. Fukui, Y. Hatsugai, and H. Suzuki, *J. Phys. Soc. Jpn.* **74**, 1674 (2005).
- [75] F. Baboux, L. Ge, T. Jacqmin, M. Biondi, E. Galopin, A. Lemaître, L. Le Gratiet, I. Sagnes, S. Schmidt, H. E. Türeci, A. Amo, and J. Bloch, *Phys. Rev. Lett.* **116**, 066402 (2016).
- [76] E. Bergholtz and Z. Liu, *Int. J. Mod. Phys. B* **27**, 1330017 (2013).
- [77] R. Barnett, *Phys. Rev. A* **88**, 063631 (2013).
- [78] A. B. Khanikaev, S. H. Mousavi, W.-K. Tse, M. Kargarian, A. H. MacDonald, and G. Shvets, *Nat. Mater.* **12**, 233239 (2013).
- [79] M. Aidelsburger, M. Lohse, C. Schweizer, M. Atala, J. T. Barreiro, S. Nascimbène, N. R. Cooper, I. Bloch, and N. Goldman, *Nat. Phys.* **11**, 162 (2015).
- [80] T. D. Stanescu, V. Galitski, J. Y. Vaishnav, C. W. Clark, and S. Das Sarma, *Phys. Rev. A* **79**, 053639 (2009).
- [81] T. Karzig, C.-E. Bardyn, N. H. Lindner, and G. Refael, *Phys. Rev. X* **5**, 031001 (2015).
- [82] A. V. Nalitov, D. D. Solnyshkov, and G. Malpuech, *Phys. Rev. Lett.* **114**, 116401 (2015).
- [83] R. Matsumoto and S. Murakami, *Phys. Rev. Lett.* **106**, 197202 (2011).
- [84] R. Matsumoto and S. Murakami, *Phys. Rev. B* **84**, 184406 (2011).
- [85] R. Matsumoto, R. Shindou, and S. Murakami, *Phys. Rev. B* **89**, 054420 (2014).
- [86] A. Mook, J. Henk, and I. Mertig, *Phys. Rev. B* **90**, 024412 (2014).
- [87] H. Lee, J. H. Han, and P. A. Lee, *Phys. Rev. B* **91**, 125413 (2015).
- [88] Y. Onose, T. Ideue, H. Katsura, Y. Shiomi, N. Nagaosa, and Y. Tokura, *Science* **329**, 297 (2010).
- [89] T. Ideue, Y. Onose, H. Katsura, Y. Shiomi, S. Ishiwata, N. Nagaosa, and Y. Tokura, *Phys. Rev. B* **85**, 134411 (2012).
- [90] M. Hirschberger, J. W. Krizan, R. J. Cava, and N. P. Ong, *Science* **348**, 106 (2015).
- [91] M. Hirschberger, R. Chisnell, Y. S. Lee, and N. P. Ong, *Phys. Rev. Lett.* **115**, 106603 (2015).
- [92] R. Chisnell, J. S. Helton, D. E. Freedman, D. K. Singh, R. I. Bewley, D. G. Nocera, and Y. S. Lee, *Phys. Rev. Lett.* **115**, 147201 (2015).
- [93] A. Mook, J. Henk, and I. Mertig, *Phys. Rev. B* **89**, 134409 (2014).
- [94] E. G. Mishchenko and O. A. Starykh, *Phys. Rev. B* **90**, 035114 (2014).
- [95] S. A. Owerre, “Magnon-mediated Hall effect in kagome antiferromagnets,” (2016), arXiv:1608.04561.
- [96] S. A. Owerre, “Topological magnon insulator in the frustrated kagome-lattice antiferromagnets,” (2016), arXiv:1609.03563.
- [97] S. A. Owerre, *J. Phys. Condens. Matter* **28**, 386001 (2016).
- [98] S. A. Owerre, *J. Appl. Phys.* **120**, 043903 (2016).
- [99] S. K. Kim, H. Ochoa, R. Zarzuela, and Y. Tserkovnyak, *Phys. Rev. Lett.* **117**, 227201 (2016).
- [100] S. A. Owerre, “Field-induced thermal Hall response in a frustrated honeycomb lattice,” (2016), arXiv:1608.00545.
- [101] S. A. Owerre, *J. Phys. Condens. Matter* **29**, 03LT01 (2017).
- [102] L. Shekhtman, O. Entin-Wohlman, and A. Aharonov, *Phys. Rev. Lett.* **69**, 836 (1992).
- [103] L. O. Manuel, C. J. Gazza, A. E. Trumper, and H. A. Ceccatto, *Phys. Rev. B* **54**, 12946 (1996).
- [104] L. Messio, O. Cépas, and C. Lhuillier, *Phys. Rev. B* **81**, 064428 (2010).
- [105] S. Okamoto, *Phys. Rev. B* **87**, 064508 (2013).
- [106] S. Okamoto, *Phys. Rev. Lett.* **110**, 066403 (2013).
- [107] M. Sigrist, D. F. Agterberg, M. H. Fischer, J. Goryo, F. Loder, S.-H. Rhim, D. Maruyama, Y. Yanase, T. Yoshida, and S. J. Youn, *J. Phys. Soc. Jpn.* **83**, 061014 (2014).
- [108] M. H. Fischer, F. Loder, and M. Sigrist, *Phys. Rev. B* **84**, 184533 (2011).
- [109] T. Watanabe, T. Yoshida, and Y. Yanase, *Phys. Rev. B* **92**, 174502 (2015).
- [110] M. Elhajal, B. Canals, and C. Lacroix, *Phys. Rev. B* **66**, 014422 (2002).
- [111] J. Colpa, *Physica A* **93**, 327 (1978).
- [112] J. van Hemmen, *Z. Phys. B* **38**, 271 (1980).
- [113] A. Sikora, H. Ftouni, J. Richard, C. Hbert, D. Eon, F. Omns, and O. Bourgeois, *Rev. Sci. Instrum.* **83**, 054902 (2012).
- [114] M. C. Wingert, Z. C. Y. Chen, S. Kwon, J. Xiang, and R. Chen, *Rev. Sci. Instrum.* **83**, 024901 (2012).
- [115] R. Schaffer, S. Bhattacharjee, and Y. B. Kim, *Phys. Rev. B* **86**, 224417 (2012).